Combustion and Flame 159 (2012) 1793–1805

Contents lists available at SciVerse ScienceDirect

Combustion and Flame

journal homepage: www.elsevier.com/locate/combustflame

A kinetic model for methyl decanoate combustion

Pascal Diévart *, Sang Hee Won, Stephen Dooley, Frederick L. Dryer, Yiguang Ju

Department of Mechanical and Aerospace Engineering, Princeton University, Princeton, NJ 08544, USA

ARTICLE INFO

Article history:
Received 18 June 2011
Received in revised form 28 July 2011
Accepted 7 January 2012
Available online 6 February 2012

Keywords:
Methyl decanoate
Biodiesel
Kinetic model
Diffusion flame
Transport-weighted enthalpy

ABSTRACT

A detailed kinetic model for the oxidation of the biodiesel surrogate, methyl decanoate, has been developed and tested against a broad range of experimental data. The methyl decanoate model consists of both low and high temperature oxidation chemistry. It has been constructed strictly through the extension of the chemical kinetic and thermochemical parameters used to describe the oxidation of the better-understood small methyl ester, methyl butanoate. The constructed model is tested in an *a priori* manner by the computation of all of the appropriate experimental data available for methyl decanoate oxidation.

The results show a generally improved performance of the present model relative to that of literature models which have generally been constructed based on similarity to alkane oxidation reaction kinetics. Chemical path flux analyses of all available methyl decanoate models are analyzed and the results reveal that the fuel oxidation pathways exhibit completely different chemical mechanisms depending on the modeling prescriptions of the kinetic and thermochemical parameters. In particular, there is a wide degree of variability in the fate prescribed to the methyl ester functionality. In addition, experimental analysis of diffusion flame extinctions for methyl butanoate and methyl decanoate reveals that the high temperature reactivity of methyl butanoate is similar to that of methyl decanoate by introducing a concept of transport-weighted enthalpy. Consequently, the present modeling work and experimental analysis suggest that further studies of small methyl ester systems, such as methyl butanoate are required in order to improve the model fidelity of large biodiesel like methyl esters.

Published by Elsevier Inc. on behalf of The Combustion Institute.

1. Introduction

Recent climate change and energy security concerns have been driving significant interests in bio-fuels such as biodiesels and alcohols that provide means to replace petroleum use and reduce net CO_2 emissions associated with transportation. Biodiesel is derived from the transesterification of triglyceride lipid with methanol (or ethanol), and is composed of a mixture of long alkyl chain methyl (or ethyl) esters. The specific molecular components and their distribution depend on the lipid source, but are limited to a small set of alkyl and alkenyl esters of 17–23 carbon atoms with zero to three unsaturations [1]. Understanding the combustion properties of these molecular structures and their interactions in blends with petroleum derived diesel fuel has been of considerable interest for the last decade. However, biodiesel compounds are difficult to study in the gas phase (fundamental fuel vapor/oxidizer experiments such as shock tube, flow reactor, jet stirred reactor, flame configurations) because of their large molecular weight and hence low vapor pressures. Thus, investigations of the kinetics of smaller molecular species that might behave combustion kinetically similar to actual biodiesel constituents have been prevalent. Such model fuels are referred to as surrogates. A surrogate fuel is either a single molecule, or a simple mixture of several molecules [2–5] that would mimic the chemical and/or the physical properties of the fuel of interest. As a result, the oxidation kinetics of a number of different esters has been studied [6–20].

Methyl butanoate, MB ($C_5H_{10}O_2$) was one of the first to be proposed to emulate biodiesel reaction kinetics. Fisher et al. [6] constructed the first detailed kinetic model by assuming similarity to the oxidation kinetics of n-alkanes. This model was later tested against experimental measurements of jet-stirred reactor (JSR), variable pressure flow reactor (VPFR), and counter-flow diffusion flame speciation profiles [7]. Recently, recognizing the uniqueness of the reactivity of the methyl ester moiety, Dooley et al. [8] further developed this MB model structure. Their model was tested comprehensively against the previous experimental data [7] and the ignition delays of MB/O_2/Diluent mixtures in both a shock tube (ST) and a rapid compression machine (RCM) over the temperature range 640–1760 K. The RCM experiments at high pressure (40 atm) confirmed JSR and flow reactor measurements that showed methyl butanoate exhibits no low temperature oxidation behavior, and thus cannot be considered as an appropriate biodiesel surrogate at low temperatures.

Consequently, more recent studies recommended larger methyl esters than MB as biodiesel surrogates to emulate the negative

* Corresponding author.
E-mail address: pdievart@princeton.edu (P. Diévart).

0010-2180/$ - see front matter Published by Elsevier Inc. on behalf of The Combustion Institute.
doi:10.1016/j.combustflame.2012.01.002

temperature coefficient (NTC) behavior of actual biodiesel. HadjAli et al. [12] studied experimentally the ignition of C_4 to C_8 methyl esters in a RCM, and then studied in more detail the behavior of methyl hexanoate ($C_7H_{14}O_2$). Dayma et al. [13] also studied this particular ester in a JSR at 10 atm and confirmed the presence of NTC behavior. Based on the kinetic model of Fisher et al., Dayma et al. developed a kinetic model of methyl hexanoate and tested it against their experimental data. More recently, experimental and modeling studies have been extended to the larger methyl esters, methyl heptanoate ($C_8H_{16}O_2$) [14], methyl octanoate ($C_9H_{18}O_2$) [15] and methyl decanoate, MD ($C_{11}H_{22}O_2$) [16–23]. Most of these kinetic models for larger methyl esters have been developed based on an assumed similarity to the oxidation kinetics of n-alkanes, for which there exists a larger reaction kinetic data base. Thus in methyl ester kinetic model development to date, there has been quite a limited focus on the specific role of the methyl ester functional group. As a result, these models occasionally over-predict the reactivity of methyl ester oxidation, in the example of MD, exhibiting shorter ignition delays (Fig. 1) and higher extinction limits of diffusion flames [9].

The previous models [16–18,21–23] of MD have been developed based on analogy to n-alkane chemistry with various modifications to rate constants relating to the reactions of the methyl ester functionality. This approach has resulted in a significant ambiguity in the description of the role of methyl ester moiety. Recent experimental studies of small methyl esters have shown clearly that fuel oxidation and CO_2 formation from methyl esters depend strongly on the particular molecular structure [24]. Therefore, an accurate kinetic model for biodiesel (or its surrogates) requires a specific knowledge of the kinetics of the methyl ester moiety. As described above, although MB does not display true low temperature reactivity, a comprehensive MB kinetic model has been developed and tested by Dooley et al. [8] resulting in relatively good agreement to a broad range of experimental data. It is logical to expect that any methyl ester specific kinetic processes are accentuated in smaller esters structures. While definite fundamental knowledge gaps certainly exist, the implication of the general reproduction of detailed experimental observations by the Dooley et al. model is that the important methyl ester specific kinetic processes have been adequately described.

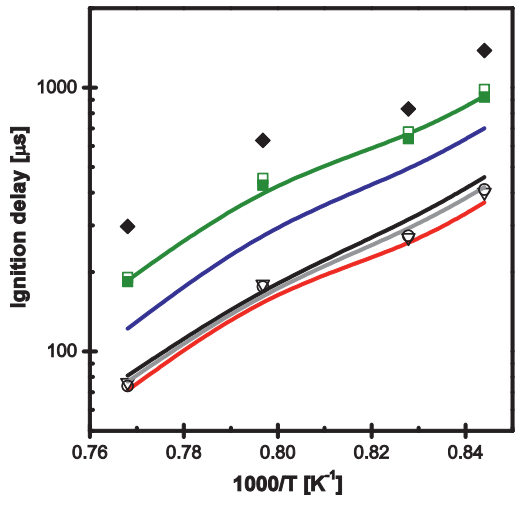

Fig. 1. Ignition delays [18] of methyl decanoate/oxygen/argon mixtures in an aerosol shock tube (♦): equivalence ratio, 0.09–0.17, fuel mole fraction, 1005–1823 ppm, and pressure, 7.57–8.03 atm. Computations with the models proposed in this study (detailed —, reduced 229 species □, reduced 529 species ■), the models of Herbinet et al. [21] (—), Herbinet et al. [22] (—), Seshadri et al. [16] (▽), Sarathy et al. [17] (—), Glaude et al. [18] (—) and Luo et al. [23] (○).

The objective of this study is to develop a kinetic model for MD, constructed by employing a similarity rule of the ester moiety from smaller methyl butanoate system to the larger MD system, and to evaluate the extent of chemical kinetic similarity between MB and MD at high temperatures. As a fundamental philosophy to model construction, we aim to utilize the rate constants and thermochemical parameter assemblies which have been derived for small methyl esters in the comprehensively tested MB kinetic model of Dooley et al. [8]. A similarity rule is applied for the estimation of rate constants and thermochemical parameters exactly as prescribed for MB to the similar MD chemistries, without any adjustment. Through this methodology, the MD kinetic model can be used to rationalize the appropriateness of the similarity rule with the hypothesis that alkyl chain length of greater than that of MB has little influence on the thermochemistry or kinetics of the ester moiety. In order to evaluate the extent of similarity in the high temperature oxidation of MB and MD a prior experimental analysis [9] is extended further. Finally, the present study evaluates and declares the fundamental knowledge gaps in methyl ester thermochemistry and reaction kinetics. The results recommend that further detailed studies on smaller methyl esters will be essential in order to construct a reliable kinetic model for bio-diesel type fuels.

2. Model construction

2.1. Methyl decanoate oxidation scheme

The kinetic model proposed here was designed from the original oxidation framework of methyl decanoate proposed by Herbinet et al. [21]. This scheme encompasses both low and high temperature kinetics of the fuel methyl ester, as well as the oxidation scheme of smaller methyl esters that may be produced from the degradation of the parent fuel. This chemical scheme was used only as a template. The rate constant parameters and thermochemical data were substituted consistently with the approach adopted in this study as described below. Necessarily, the oxidation kinetic of the smaller species (C_0—C_5) was updated according to the recent work of Healy et al. [25].

2.2. Thermochemical data

A few recent studies deal with the estimation of the thermochemical properties of methyl (and ethyl) ester species. El-Nahas et al. [26] determined the Bond Dissociations Energies (BDEs) of MB and Ethyl Propanoate (EP) through *ab initio* computations (complete basis set method CBS-QB3). Osmont et al. [27,28] proposed a new computational approach to estimate the enthalpy of formation of a large set of hydrocarbons, including large methyl esters. Both groups derived the BDEs of the methyl (ethyl) ester moiety from their computational results. Sumathi and Green [29] worked on oxygenated fuels (alcohols, esters, ethers and carboxylic acids) and proposed new estimates for methyl ester group contributions, derived from *ab initio* computations (complete basis set method CBS-Q). The BDEs proposed by these three groups are presented in Table 1. Reasonable consistency, within 2–3 kcal mol^{-1}, is observed between the studies, but some important uncertainties and significant differences to equivalent alkane parameters are apparent. Especially, the C—H BDE of the methyl ester group falls in the range 98.95–100.5 kcal mol^{-1}, which is lower by 0.7–2.2 kcal mol^{-1} than a primary C—H bond as in n-alkanes. The BDE of the C—H bond α to the carbonyl position has a value (92.0–94.2 kcal mol^{-1}) intermediate between that of a secondary C—H bond (~98.5 kcal mol^{-1}) and a secondary allylic C—H bond (~85.6 kcal mol^{-1}). A greater consensus of the thermochemical

Table 1
Methyl Decanoate Bond Dissociation Energies at 298.15 K: comparison between this study, computational values and available literature kinetic models (units: kcal mol^{-1}).

Bond	El Nahas et al. [26] (MB)	Osmont et al. [27,28]	Sumathi et al. [29]	Present model (MB)	Present model (MD)	Herbinet et al. [21] Version 1a	Sarathy et al. [17]	Herbinet et al. [22] Version 2	Seshadri et al. [16]	Luo et al. [23]	Glaude et al. [18]	Dooley et al. [8] (MB)
RCO_2CH_2—H	98.9	99.3	100.5	100.3	100.0	100.3	100.3	100.3	100.3	/	99.0	100.0
RCO_2—CH_3	87.0		/	86.7	86.8	86.9	86.9	86.9	86.9	86.9	85.7	86.8
RCO—OCH_3	101.3	/	/	99.1	99.2	99.1	99.1	99.1	99.1		97.8	99.2
R—CO_2CH_3	93.5	/	/	92.3	91.9	93.0	93.0	93.0	93.0	93.0	93.9	89.9
H_3CO_2CH(R)—H	94.2	92.0	/	93.6	93.6	94.1	94.1	94.1	94.1	94.1	94.3	93.6
R—$CH_2CO_2CH_3$	84.4	82.9	/	85.9	85.6	85.2	85.2	80.9	80.9	80.9	83.5	85.2

properties of methyl ester fuel and of the oxygenated species involved in the kinetic model is thus required, as these inputs strongly affect the kinetic parameters. The thermochemical data of the species involved in the methyl decanoate reaction set (from methyl pentanoate to methyl decanoate, such as to be consistent with the smaller methyl esters from the methyl butanoate submodel) were estimated by the group additivity method proposed by Benson [30] and as implemented in the software THERM. [31]. Group contributions for the ester groups were chosen consistently with those employed by Dooley et al. [8], taken mostly from Sumathi and Green [29].

Figure 2 shows the BDEs which result from these estimates. Table 1 shows a comparison between these BDEs and those employed in previous kinetic models. The BDEs computed for MB and MD with the present model are consistent with each other. The small discrepancies (about 0.4 kcal mol^{-1}) can be attributed to uncertainties associated with the estimation of the enthalpies of formation of large 1-alkyl radical through the group additivity method. The BDEs calculated with the present model for methyl decanoate are consistent with those determined by El-Nahas et al. [26] for MB (within 2% difference). The values are also consistent with those computed from the first version of the methyl decanoate model of Herbinet et al. [21]. However, the model of Glaude and co-workers [18] prescribed generally lower BDEs than the other models. It should also be noted that the second version of the methyl decanoate model of Herbinet et al., the models of Luo et al. [23] and Seshadri et al. [16] suggest an extremely low BDE value of the bond between the α and β carbon atoms. Such a low value implies that the rate constant computed for the unimolecular fuel decomposition (UFD) reaction associated to this bond is very high and may increase the oxidation rate of the fuel substantially.

2.3. Kinetic parameters

Different MB oxidation models (e.g., Fisher et al. [6], Hakka et al. [11] and Dooley et al. [8]) have been proposed in the literature. These models were tested against different experimental data sets. All of them have different prescriptions for the BDEs of methyl ester species, but also use different kinetic parameter sets for the key reactions of methyl ester oxidation. Especially, the hydrogen abstraction rate constants from the position α to the carbonyl (*i.e.*, methyl ester specific) are widely inconsistent. Herein, the "branching ratio" is defined as the ratio between the rate constant

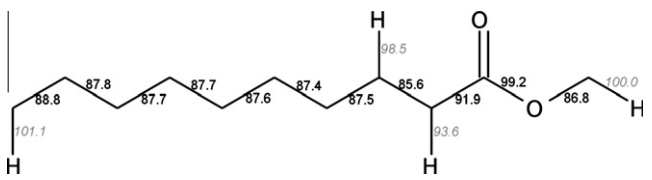

Fig. 2. Bond Dissociation Energies (BDEs) (black: C—C bonds; gray, C—H bonds) calculated at 298.15 K for methyl decanoate (unit: kcal mol^{-1}).

of hydrogen abstraction reaction by a radical X on the position of interest over the sum of the individual rate constants for hydrogen abstraction from the fuel by this radical. The branching ratio for the H abstraction reactions on these methyl ester specific positions as a function of the temperature is shown in Fig. 3. This plot shows a large variability between the three models for the propensity for hydrogen atom abstraction on the methyl ester carbon. Fisher et al. (also adopted by Herbinet et al. [21] for MD) assumed that this position is similar to a primary carbon atom, and so did not consider any weakening of the BDE relative to the analogous position in propane. Dooley et al. evaluated the works of Sumathi and Green [29] and El-Nahas et al. [26] and accounted for this particularity by proposing rate constants that enhance the branching ratio for this position. The values nominated by Hakka et al. [11] are of intermediate value between those of the aforementioned models. A similar review is also presented for the β-scission reactions and the UFD reactions involving the ester moiety. Large disparities are observed between the different models for the formation of formaldehyde from the $C_3H_7CO_2CH_2$ radical (MBMJ). Attempting to account for the uniqueness of this process, Dooley and co-workers have proposed a higher decomposition rate constant than Fisher et al. [6] and Hakka et al. [11]. Previous studies have shown that the formation of formaldehyde in the oxidation of methyl esters plays a significant role in regulating diffusion flame extinction, indicating that an accurate description of this process should be targeted [9] for model improvement.

Accounting for these previous observations and considering the experimental validation range, the work of Dooley et al. [8] has been adopted as a base model for this study. Thus the MB subset has been added to the set of reactions described above.

The kinetic parameters proposed by Dooley et al. for methyl butanoate oxidation were prescribed on a reaction by reaction basis to analogous reactions in the oxidation scheme of methyl decanoate and all of the smaller methyl ester species. The reaction classes modified are:

(1) Hydrogen abstraction reactions from the fuel and stable intermediates (Table 2).
(2) Isomerization reactions of methyl esters alkyl radicals.
(3) β-scission reactions of the methyl ester alkyl radicals, and
(4) Unimolecular fuel decomposition reactions (UFD).

For reaction classes three and four, the rate constant parameters prescribed by Dooley et al. are those of the reverse reactions. We follow the same approach with the forward rate constants computed from microscopic reversibility and thus also testing the assigned thermochemistry. Moreover, to be fully consistent with the approach of Dooley et al., the UFD reactions were treated through quantum Rice–Ramsperger–Kassel theory with a master equation analysis [32,33]. The resulting rate constant expressions were fitted in the Troe formalism to be used for modeling. This pressure dependence correction strongly impacts the rate constant. The rate constants for the high-pressure limit relative to

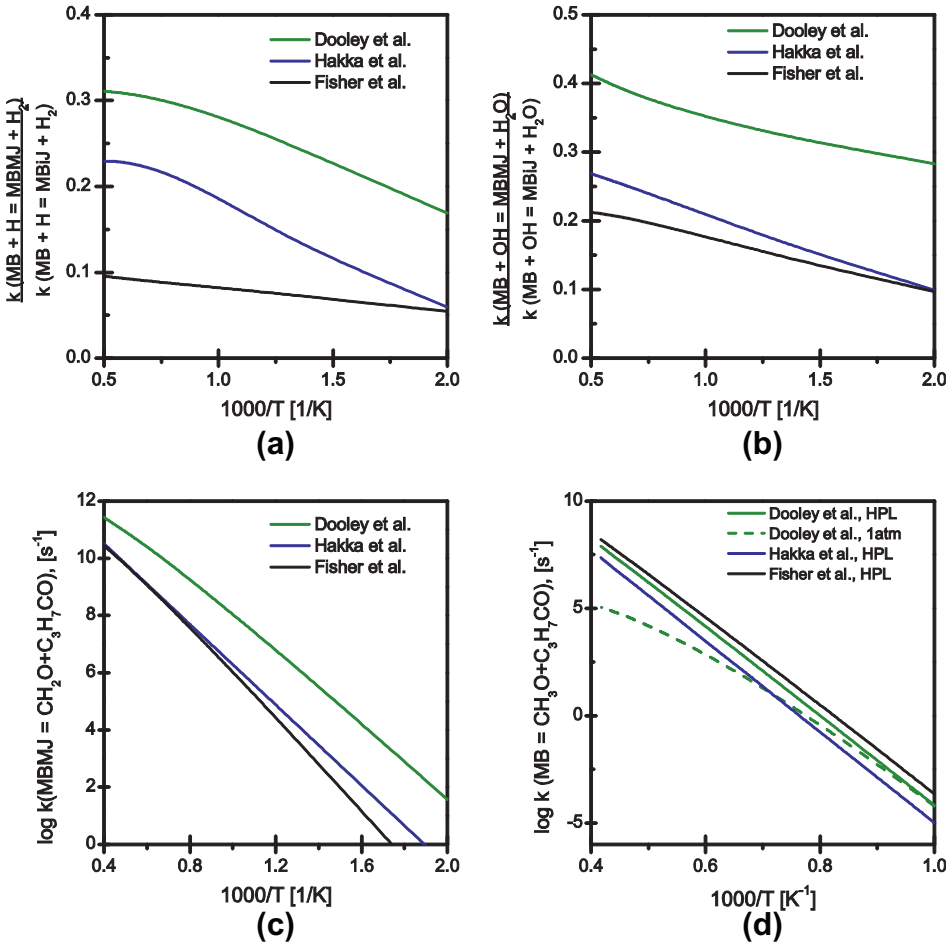

Fig. 3. Branching ratio of methyl butanoate with H atoms (a) and OH radicals (b), rate constant of the MBMJ ($C_3H_7CO_2CH_2$) radical β-scission reaction (c) and unimolecular methyl butanoate decomposition reaction to CH_3O and C_3H_7CO radical (d) in the models of Dooley et al. [8] (—), Hakka et al. [11] (—) and Fisher et al. [6] (—).

Table 2
H abstraction rate constant parameters (k = A x T^n x exp(-E/RT); A, E; units: $cm^3\ mol^{-1}\ s^{-1}$ and $cal\ mol^{-1}$) by the main radicals adopted in the present kinetic model and in the Herbinet et al's model [21].

Radical	MD + X = MDMJ + HX				MD + X = MD2J + HX			MD + X = MDiJ + HX (i = 3,. . .,9)			MD + X = MD10J + HX		
		A	n	E	A	n	E	A	n	E	A	n	E
OH	Herbinet et al.	5.27×10^9	0.9715	90	1.15×10^{11}	0.51	63	4.67×10^7	1.61	-35	5.27×10^9	0.97	1590
	Present model	7.02×10^7	1.61	-35	1.15×10^{11}	0.51	63	4.68×10^7	1.61	-35	5.28×10^9	0.97	1586
H	Herbinet et al.	9.40×10^4	2.7562	80	3.62×10^6	2.54	6756	1.30×10^6	2.40	4471	9.40×10^4	2.75	6280
	Present model	1.95×10^6	2.4044	71	1.20×10^6	2.40	2583	1.30×10^6	2.40	4471	6.60×10^5	2.54	6756
HO_2	Herbinet et al.	4.05×10^4	2.50	16690	7.22×10^3	2.55	10530	5.88×10^4	2.50	14860	4.05×10^4	2.50	16690
	Present model	1.23×10^4	2.60	13910	6.14×10^3	2.55	10530	8.19×10^3	2.60	13910	2.02×10^4	2.55	16490
O	Herbinet et al.	1.05×10^6	2.4247	66	3.94×10^5	2.40	1150	5.95×10^5	2.44	2846	1.05×10^6	2.42	4766
	Present model	8.28×10^5	2.4528	30	7.66×10^5	2.41	1140	5.52×10^5	2.45	2830	9.81×10^5	2.43	4750
CH_3	Herbinet et al.	4.52×10^{-1}	3.6571	54	2.72	3.65	7154	8.40×10^4	2.13	7574	4.52×10^{-1}	3.65	7154
	Present model	2.27	3.4654	81	1.20×10^{-9}	6.36	89	1.51	3.46	5481	4.53×10^{-1}	3.65	7154

the QRRK estimated rate constant at atmospheric pressure are decreased by approximately a factor of three at 1000 K and a factor of twenty at 1500 K.

However, the rate constant parameters associated to the low temperature oxidation chemistry of n-alkanes and methyl butanoate are recognized as being uncertain, and new rate constant estimates have been or are about to be proposed [34–37]. To be consistent with the goals of this study, the low temperature kinetic parameters were retained from the initial model of Herbinet et al. [21]. However it is noted that preliminary tests with up-to-date kinetic parameters for the generic low temperature scheme have shown an enhancement of the fuel reactivity at the end of the NTC region.

2.4. Transport data

The Lennard–Jones (LJ) parameters (σ and ε/k) of methyl ester species were estimated according to Dooley et al. [9]. The dipole moment was chosen equal to 1.7 D [38] and the polarizability calculated according to Bosque and Sales [39]. The different sets of transport coefficients for MD available from previous modeling works are presented in Table 3. The coefficients proposed here are

Table 3
Comparison between the transport parameters adopted for methyl decanoate in this study and in the kinetic models available in the literature.

Study	σ (Å)	ε/k (K)	μ (D)	α (Å^3)	Comment
Present study	6.934	587	1.70	21.90	LJ parameters estimated from a molecular weight correlation [9]
Seshadri et al. [16]	7.305	604.4	1.70	0.0	Tee, Gotoh and Stewart method T_c and P_c taken equal as those of species with similar size and structure
Luo et al. [23], Sarathy et al. [17]	6.807	636.2	1.70	21.69	Tee, Gotoh and Stewart method T_c and P_c estimated by extrapolation of critical properties of smaller esters
Wang et al. [10]	7.040	788.0	/	/	Tee, Gotoh and Stewart method T_c and P_c estimated by Joback's group additivity method

in reasonable agreement with those proposed in previous studies, the main difference is observed on the well-depth potential (25% difference with the value suggested by Wang et al. [10]). However, the collision diameter is the main parameter governing the binary diffusion coefficient, and Fig. 4 shows that the computed binary diffusion coefficient $D_{MD,N2}$ are consistent between the different transport datasets. Therefore, any deviations in one dimensional configuration between two models can be related to differences in either the thermochemistry or the kinetics employed.

2.5. Model reduction

The detailed model involving 2276 species in 7086 reactions is too large to be used for flame simulations. The multi-generation Pathway Flux Analysis (PFA) method, as implemented in the Princeton Chem-RC software [40], was used to reduce the size of the model. Two reduced models were generated. The largest one (530 species and 2396 reactions) was validated successfully against the detailed model and used to compute the laminar flame speeds. The smaller reduced model (238 species and 1244 reactions) is used to compute the series of diffusion flames that result in the determination of the extinction strain rate. Both reduced models are in good agreement with each other and experiments for premixed flame conditions, high temperature ignition delay and stirred reactor speciation. A comparison between the detailed models and the two reduced models is available in the Supplementary materials.

2.6. Modeling methods

The model described above has been tested against shock tube ignition delays, JSR speciation, diffusion flame speciation, laminar flame velocities and against the extinction limits of diffusion flames. The PSR [41] and SENKIN [42] modules of the CHEMKIN II package [43] were respectively used to model the experiments in JSR and shock tube (exercising both constant volume and variable volume assumptions). The counterflow flame simulations were performed with the OPPDIFF code [44] from the CHEMKIN III package utilizing mixture averaged transport. Flame velocities were computed with both Premix [45] and Cantera [46] utilizing multicomponent transport descriptions, the solutions of both codes are extremely similar.

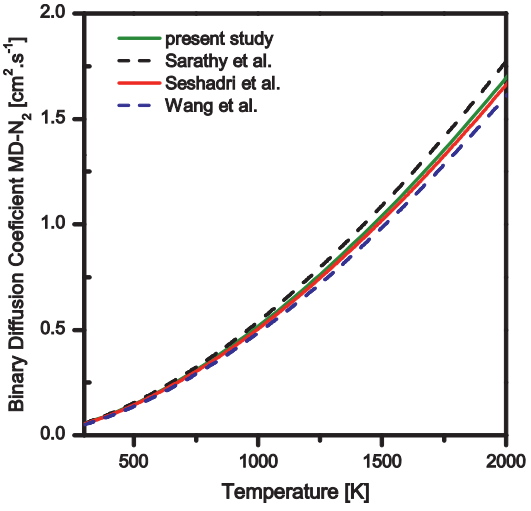

Fig. 4. Binary diffusion coefficients of methyl decanoate-N_2 as a function of temperature, computed using the Lennard–Jones parameters proposed in this study, by Seshadri et al. [16], Sarathy et al. [17] and Wang et al. [10].

3. Model predictions against available experimental data

3.1. Low to intermediate temperature oxidation

3.1.1. Ignition delays

Wang and Oehlschlaeger [20] have recently measured the ignition delays of MD/air mixtures for three different equivalence ratios ($\varphi = 0.5$, 1.0 and 1.5) in a shock tube at 16 atm. They investigated a broad range of initial temperatures, observing NTC behavior for MD ignition delay. Figure 5 shows the modeling computations with the present model, the model of Glaude et al. [18], and the model of Herbinet et al. [21] with the experimental data for the stoichiometric mixture. The model of Glaude et al. under estimates the ignition delays in the NTC region, and over predicts the ignition delays at higher temperature. As pointed out by Wang and Oehlschlaeger, the model of Herbinet et al. is in relatively good agreement with the experimental data. The present model also

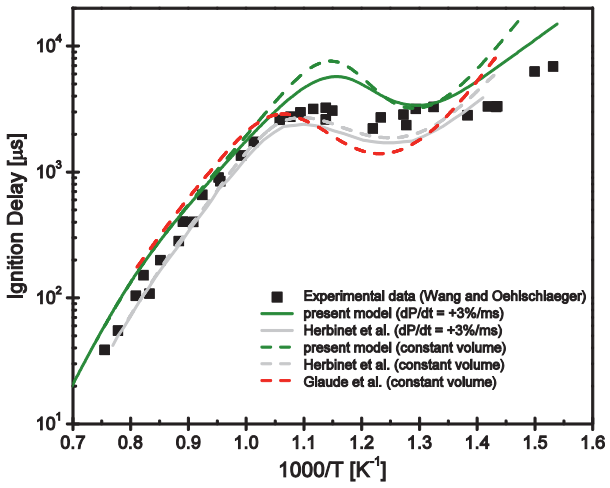

Fig. 5. Ignition delays of stoichiometric MD/air mixtures at $P \sim 16$ atm. The symbols are the experimental data [20], the green line the present model, the black line is the model of Herbinet et al. [21] and the blue line the model of Glaude et al. [18]. Computations were run with a variable volume history (solid lines, $dP/dt = +3\%/ms$ as reported in [20]) or with a constant volume (dash lines). (For interpretation of the references to color in this figure legend, the reader is referred to the web version of this article.)

shows quite good agreement at high temperatures but over estimates the ignition delays of the lower temperature regime. The deficiency of the present model for the low temperature regime may be attributed to the following reasons.

Firstly, although the low temperature oxidation scheme of the present model was directly adopted from Herbinet et al., the thermochemical data of the low temperature related species have been re-estimated in the present model. The same additivity groups as used for the high temperature related species were also adopted in order to maintain the consistency throughout the model. Since the low temperature ignition is strongly controlled by the chemistry of the peroxy alkyl RO_2 species, the formation of these species and their subsequent reactions (isomerization, second O_2 addition) are governed by chemical equilibrium and are thus highly dependent on thermochemical data. Therefore, the modification of the thermochemical properties results in the change of chemical equilibrium in spite of keeping the same forward rate constant suggested by Herbinet et al. Consequently, the present model exhibits somewhat different performance at low temperatures compared to the model of Herbinet et al.

Secondly, the present MD kinetics has been written strictly by propagating the methyl butanoate kinetics as a model molecule. The previous experimental studies have shown that the MB does not exhibit low temperature reactivity [7,8,11] clearly shown for MD ignition delay in Fig. 5. Thus, it can be regarded that the low temperature chemistry implemented in the present MD model requires further detailed studies in order to improve the model fidelity. Moreover, recent studies [34–37] aimed at computing and refining the kinetic parameters associated with the low temperature oxidation of n-alkanes indicate that important uncertainties still exist in those submodels. Although the present model shows reasonable agreement against the relatively limit range of low temperature oxidation measurements for MD, an improved quantitative fundamental understanding of the low temperature reaction kinetics of both n-alkanes and methyl esters is required.

3.1.2. Jet-stirred reactor

Glaude et al. [18] studied the oxidation of a methyl decanoate/O_2/He mixture in a JSR at atmospheric pressure, between 500 and 1100 K. This study provided speciation data for the low-temperature oxidation of methyl decanoate (reactants, products and main intermediates). However, the authors could not detect and quantify formaldehyde, which is one of the main intermediate species most specific to the methyl ester oxidation chemistry. Figure 6 presents a comparison between the present detailed model, the model of Sarathy et al. [17], the model of Glaude et al. [18], the model of Herbinet et al. [21] and the experimental data. The present detailed model is in overall good agreement with the experimental data. The main differences between all the models are observed for ethylene, methyl acrylate ($C_2H_3CO_2CH_3$) and formaldehyde (Fig. 7). These differences are important as ethylene and formaldehyde are identified controlling intermediates in many combustion kinetic phenomena, and methyl acrylate and formaldehyde are intermediate species that result from oxidation pathways directly attributable to the methyl ester functionality. The model of Glaude et al. computes the lowest methyl acrylate concentration (close to experimental profiles, Fig. 8h), whereas all other models forecast large amounts of this unsaturated ester. However the Glaude et al. model also computes significantly higher mole fraction of formaldehyde, ~70% higher than all the other models. The formation of ethylene is related to the decomposition of the alkyl chain of the methyl ester, and for a molecule with such a large alkyl chain, ethylene production ought to be influenced very little by processes specific to the ester moiety [9]. The discrepancies observed for the ethylene fractions computed by each model may be ascribed to the different C_0—C_3 subsets (and therefore to the

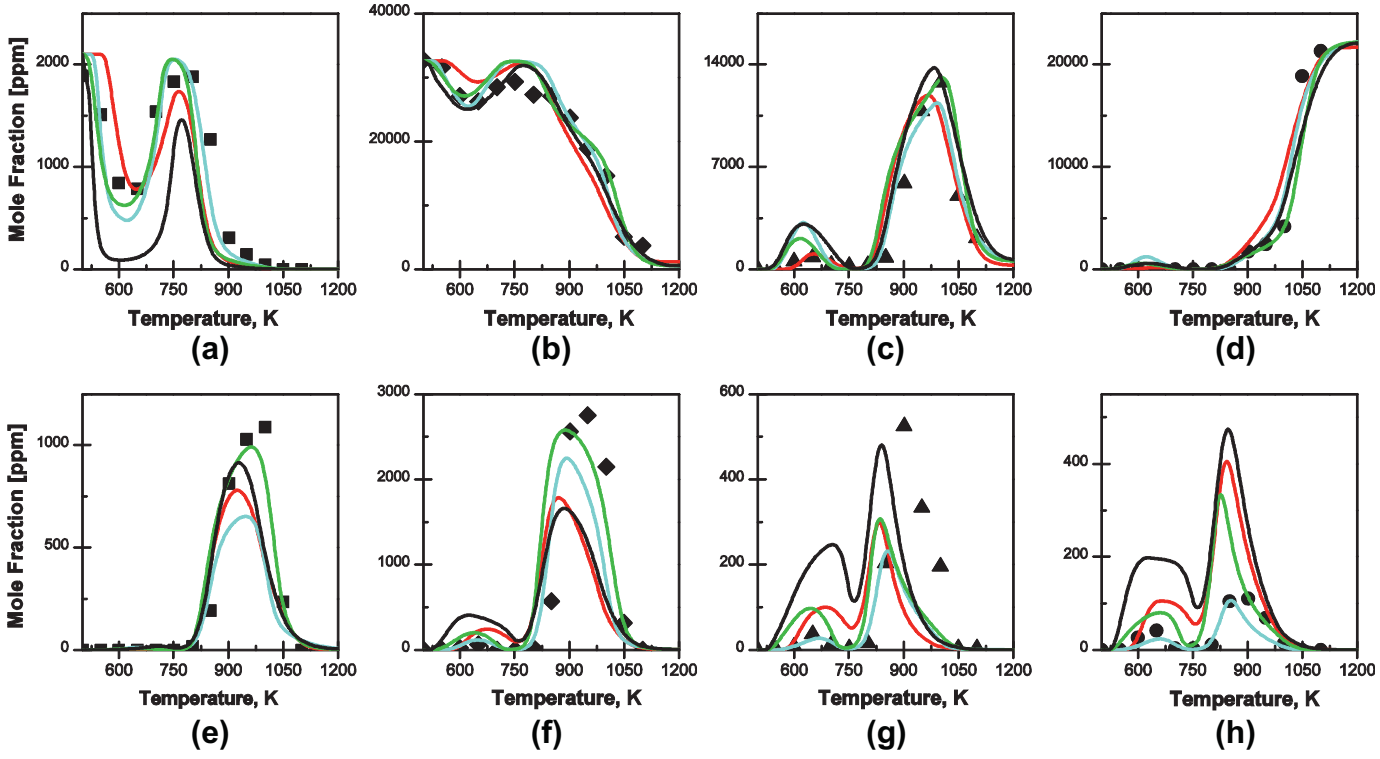

Fig. 6. Oxidation of a stoichiometric methyl decanoate/oxygen/helium mixture of 2100/32,550/965,350 ppm in a jet stirred reactor at 1 atm and a residence time of 1.5 s. Experimental data [18] (symbols) and model computations (lines): the present detailed model (—), Sarathy et al. [17] (—), Herbinet et al. [21] (—) and Glaude et al. [18] (—): MD (a), O_2 (b), CO (c), CO_2 (d), CH_4 (e), C_2H_4 (f), C_3H_6 (g) and methyl acrylate (h).

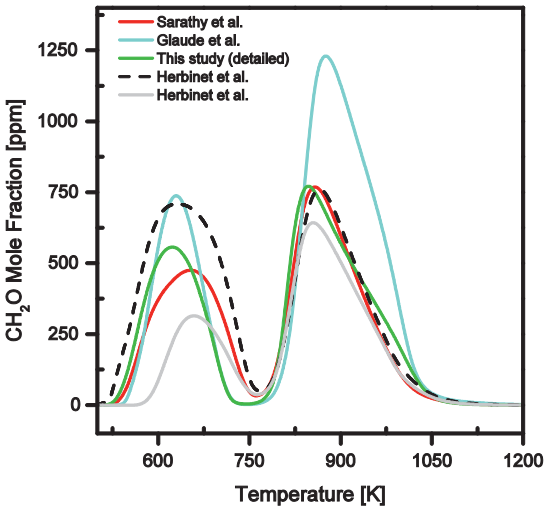

Fig. 7. Formaldehyde mole fraction computed by different models in a JSR (P = 1 atm, 2100/32,550/965,350 ppm methyl decanoate/oxygen/helium mixture, φ = 1.0, τ = 1.5 s).

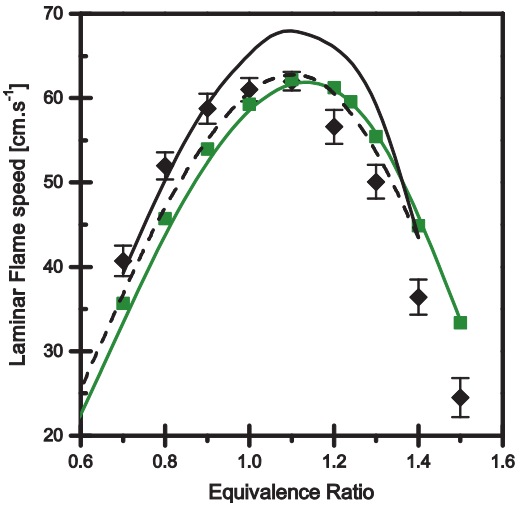

Fig. 8. Flame speed of methyl decanoate/air mixtures at atmospheric pressure and 403 K. Experimental data from Wang et al. [10] (♦), reduced model 529 species (■), reduced model 228 species (—), Seshadri et al. [16] (—) and Luo et al. [23] (- - -).

consumption reactions of C_2H_4) adopted [47]. However, the large deviations observed in the computations of methyl acrylate and formaldehyde profiles are governed by the kinetics of the methyl ester group.

The modification of the thermochemical data for low temperature related species are found to strongly affect the low temperature profiles of the fuel and small unsaturated species (C_2H_4, C_3H_6 and methyl acrylate). As an example, the model of Herbinet et al. computes about 95% of the fuel to be converted at the studied residence time of 1.5 s and at the temperature of 620 K, whereas the present detailed model only computes 75%, which is in closer agreement with the conversion yield experimentally measured. These observations are consistent with the results shown in Figs. 1 and 5. The model of Herbinet et al. was found to show the fastest rate of oxidation, whereas the present model was found to show amongst the slowest rate of oxidation and is the slowest in terms of ignition delay.

3.2. High temperature oxidation

3.2.1. Ignition delays

Haylett et al. [19] have measured the ignition delays of methyl decanoate/O_2/Ar mixtures in an aerosol shock tube. Very fuel lean mixtures (equivalence ratio 0.09–0.17) were investigated at intermediate temperatures (1125–1350 K) and pressures (~7 atm). Model computations with the models of this study and previously published MD models against experimental data are presented in Fig. 1.

The different reduced models derived from the detailed model of the present study show consistent computed ignition delays. All the models evolving from the work of Herbinet (*i.e.*, Herbinet et al. [21,22], Seshadri et al. [16], Sarathy et al. [17] and Luo et al. [23]) strongly overestimate the oxidation rate, and compute ignition delays that are lower by about 80% than experimentally measured. The model of Glaude et al. [18] is in better agreement but still under-predicts the ignition delays by ~50%. The present model also under-predicts the ignition delays but modestly, at an average deviation of 35%, and thus shows considerably closer agreement than the aforementioned models.

3.2.2. Laminar burning velocities

Wang et al. [10] have determined the laminar burning velocity of methyl decanoate/air mixtures at atmospheric pressure and initial temperature of 403 K with a counterflow burner. Figure 8 presents the experimental data of Wang et al. along with the computations from different models: the two reduced models proposed in this study, the reduced model of Seshadri et al. [16] and the reduced model of Luo et al. [23]. Both reduced models proposed in this study are in a very good quantitative agreement ($S_{L,max}$ is computed to be 62.3 cm s^{-1} whereas it is experimentally 62.0 cm s^{-1}) but compute a maximum flame speed peak slightly shifted to higher equivalence ratio (by about 0.05). As a result, the model overestimates the experimental data in fuel-rich conditions whereas the laminar burning velocities in fuel-lean conditions are underestimated.

3.2.3. Diffusion flame – extinction Limits

Dooley et al. [9] reported diffusion flame extinction limits, a_E, as a function of fuel mole fraction of methyl butanoate, n-heptane and methyl decanoate diffusion flames in a counterflow facility at atmospheric pressure. The fuel stream temperature was fixed at 500 K for both hydrocarbons and the oxidizer stream was held at 298 K. Figure 9 presents these experimental data and the computed (mixture-average transport) extinction limits with the present reduced model (228 species) for both MB and MD (a reduced model for MB has been generated by the same approach from the detailed MD model). The computations with the models of Seshadri et al. [16] (derived from the first version of the model of Herbinet et al. [21]) and Luo et al. [23] (derived from the second version of the model of Herbinet et al. [22]) are also shown. The detailed models of Herbinet et al. [21,22] and the model of Glaude et al. [18], involving hundreds of species and thousands of reactions, were too large to compute the necessary series of one dimensional simulations that result in the extinction limit. Therefore no computations of these models are presented at the diffusion flame condition. From Fig. 9 the model of Seshadri et al. overestimates the extinction strain rates, whereas the model of Luo et al. [23] is in much better agreement. The present reduced model computes extinction limits in very close agreement with those of the model of Luo et al. and with experiment.

The methyl butanoate (MB) model computations exhibit very similar behavior to the computations of the MD model against extinction strain rate. The model captures reasonably well the experimental data for the lowest fuel mole fraction, but underestimates the extinction limit as the fuel mole fraction increases. The model performs very well in the computation of n-heptane

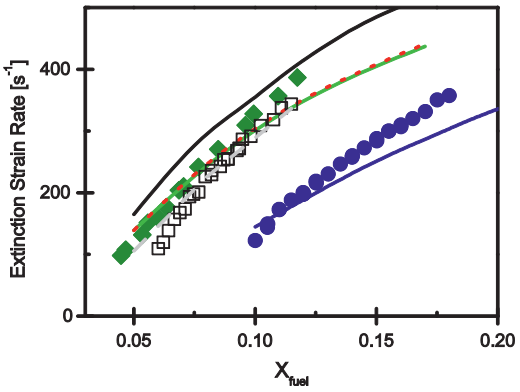

Fig. 9. Extinction strain rates of methyl decanoate/air diffusion flames at. $T = 500$ K (◆), methyl butanoate/air (●) and n-heptane (□) [9] diffusion flames at $T = 500$ K. Lines are modeling computations: this study MD (—), this study MB (—), this study nH (— —), Seshadri et al. [16] (—) and Luo et al. [23] (- - -).

extinction limits, no such discrepancies are observed at the largest fuel fraction. The high temperature kinetics applicable to n-alkyl functionalities as implemented in the present model is thus reliable. Therefore, the discrepancies observed for the high temperature oxidation of MD can likely be attributed to uncertainties associated with the thermochemical and kinetic properties prescribed to the methyl ester moiety as suggested in our previous work [9]. Moreover Fig. 9 also suggests that any discrepancy observed in the computation of MB extinction propagates to the similar MD computations when the present modeling methodology is applied. As a consequence, an improved mechanistic and quantitative kinetic comprehension of the kinetics of smaller methyl esters such as MB and its main intermediates is a primary target before moving towards larger methyl esters.

3.2.4. Diffusion flame speciation

Sarathy et al. [17] have published speciation data of a methyl decanoate/O_2/N_2 diffusion flame. They identified and quantified reactants, products and major intermediate species, except unsaturated methyl esters. The comparison between the present reduced model (229 species) and the models of Sarathy et al. [17], Seshadri et al. [16] and Luo et al. [23] against experimental data are presented in Fig. 10.

All the models exhibit negligible differences in the computation of the temperature profile and the concentration profiles of reactants (MD) and oxidation products (CO_2 and CO). However, the computed profiles for small intermediate species, especially oxygenates (formaldehyde, ketene), are found to be very different between all tested models. The four models fail to reproduce the rate of consumption of methyl decanoate. The systematic discrepancy between experimental and computed profiles for the fuel in opposed diffusion flame may be due in some significant part to non-ideal flow velocity profiles at the exit of the nozzles which are not described by the physical simulation model [48]. However, all models perform well in capturing the spatial evolution of intermediate species. The present model computes the lowest maximum formaldehyde mole fraction, but still over predicts the experimental data by a factor of two (the model of Luo et al. shows the most extreme deviation at a factor three higher than experiment). A different behavior is observed for the ketene profile: the present model computes the highest mole fraction (a factor of two higher than that computed by the models of Sarathy et al. and Seshadri et al.). The large discrepancy between the kinetic models and the formaldehyde experimental data has been previously pointed out by the Sarathy et al. They suggested that sampling issues may explain this observation: formaldehyde may polymerize in the sampling probe resulting in a lower concentration in the sample gases. Nonetheless, the lack of reliable quantitative data of this intermediate species is limiting to the accuracy of methyl ester combustion models.

3.3. Path flux analysis

The previous section presented the overall performance of the proposed MD model against experimental data and previous models computations. In this section, reaction pathway analyses have

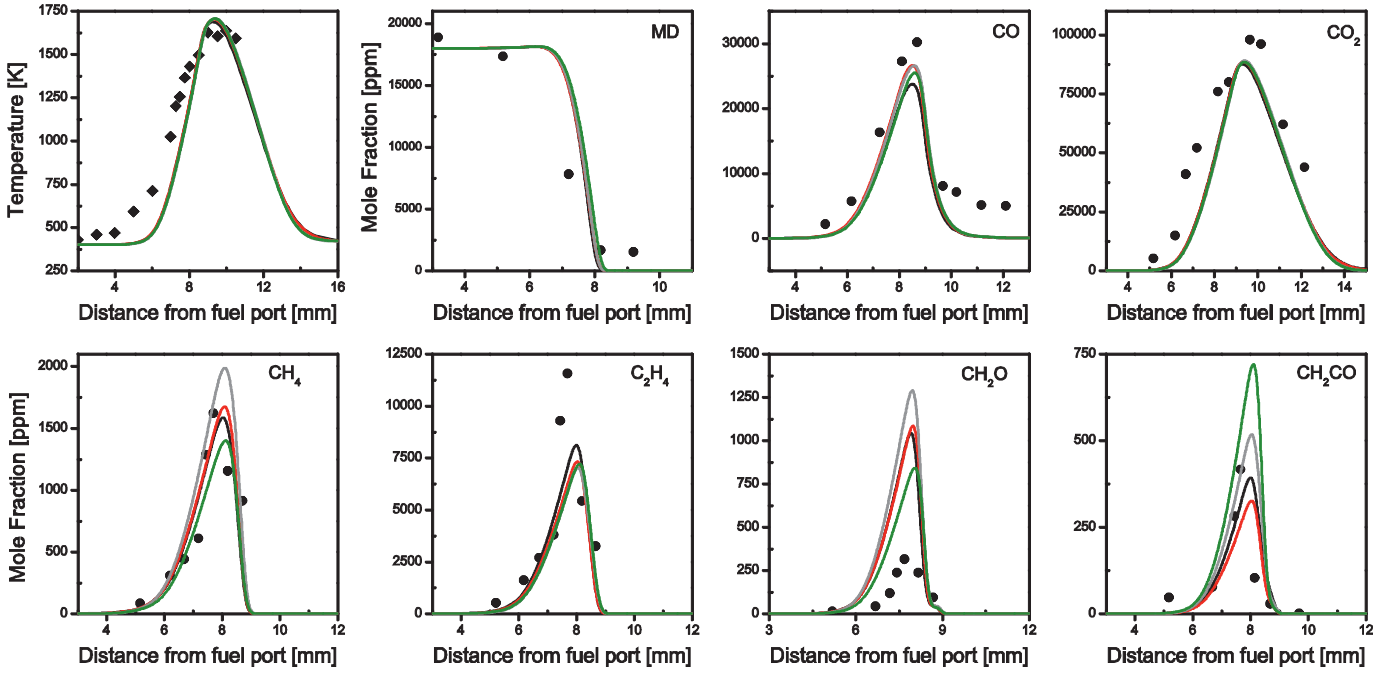

Fig. 10. Species and temperature profiles from methyl decanoate oxidation in an atmospheric pressure diffusion flame (MD: 1.8%, O_2: 42%, $a = 31$ s^{-1}). Symbols are experimental data [17], solid lines are computations (solving the gas energy equation) with the present reduced model (229 species, —), the model of Sarathy et al. [17] (—), the model of Luo et al. [23] (—) and the model of Seshadri et al. [16] (—).

been performed for selected combustion conditions to identify and point out the differences in the initial MD oxidation paths forecasted by the different models.

3.3.1. MD oxidation at intermediate temperatures and very fuel lean mixtures (ϕ = 0.09–0.17)

The first configuration investigated is a constant volume, constant internal energy auto-ignition simulation. An overall pathway analysis with all the MD models has been performed in the thermodynamic conditions studied experimentally by Haylett et al. [19] (ϕ = 0.09–0.17, P ≈ 8 atm, 1185 K < T < 1302 K). Regardless of the model, the parent fuel reacts mainly (>90%) through H atom abstraction reactions with OH radicals and H atoms as the main abstractors. The fuel fraction that decomposes through UFD reactions is found to be strongly dependent on the various BDEs prescribed in the models. The models with the lowest BDEs (Herbinet et al. [22], Seshadri et al. [16], Luo et al. [23]) compute the largest proportion of UFD (∼9%, with a predominance for the reaction producing the 1-octyl and CH_3OCOCH_2 radicals). In contrast the present model predicts only ∼2% of total fuel consumption through this reaction class.

A more detailed path flux analysis (1185 K, 7.84 atm, 50% fuel conversion) with three different detailed models (the present detailed model, the model of Herbinet et al. [21] and the model of Glaude et al. [18]) is presented in Fig. 11. The initial distribution among MD radicals is computed differently by all the models. Firstly, the model of Herbinet et al. computes a small amount of the two radicals most specific to the methyl ester functionality (MD2J ($CH_3(CH_2)_7CHCO_2CH_3$) and MDMJ ($C_9H_{19}CO_2CH_2$)). Conversely, more than 25% of the parent fuel is converted to these two radicals in the model of Glaude et al. and in the present model (with a stronger preference to MDMJ relative to the model of Glaude et al.). However the two models compute different consumption paths for these methyl ester specific radicals. The model of Glaude et al. emphasizes the isomerization reactions over the β-scission reactions, whereas in the present model, MD radicals exclusively decompose through β-scission reactions. Thus different overall reactivity is computed by each model. This analysis demonstrates that the branching ratio between β-scission and isomerization reactions specific to these methyl ester radicals needs further investigation in order to reproduce both global oxidation parameters and speciation data.

3.3.2. MD oxidation in a counter-flow diffusion flame

The second configuration investigated is the opposed diffusion flame (fuel/N_2 mixture at the fuel side, air at the oxidizer side). Figure 12 presents an overview of the fuel consumption pathways with the present reduced model and the models of Luo et al. [23] and Seshadri et al. [16]. From Fig. 12, all models show MD to react mainly through H abstraction reactions. The main abstracting radical in all three models is H atom, followed by OH radical. It is noteworthy that the proportion of MD reacting with OH increases with the strain rate as we have suggested previously [9]. However the yield of the UFDs is widely different between the present model and the models derived from Herbinet et al., though it is noted that all models show this reaction class to become less prominent as the flame is closer to extinction. A fundamental analysis rationalizing this behavior has been presented previously [9]. In the models of Luo et al. and Seshadri et al. up to 50% of the fuel may break down unimolecularly, whereas the model of the present study computes a maximum yield of 10% for this reaction class. The detailed path flux analysis shows that the reaction producing the $CH_2C(O)OCH_3$ (ME2J) and 1-octyl radicals from the fuel is again the most prominent (up to 35% of the fuel consumption). The rate constant of this reaction has been previously reported [22] to be overestimated in the models of Herbinet et al. (due to the low BDE prescribed). The large deviation between the reaction yields of MD between the present model and the model of Luo et al. is surprising as both models compute similar extinction limits.

In Fig. 13 the initial distribution between the MD radicals is computed to be different between the present model and the model of Seshadri et al. [16] (the lumping of all methyl decanoate

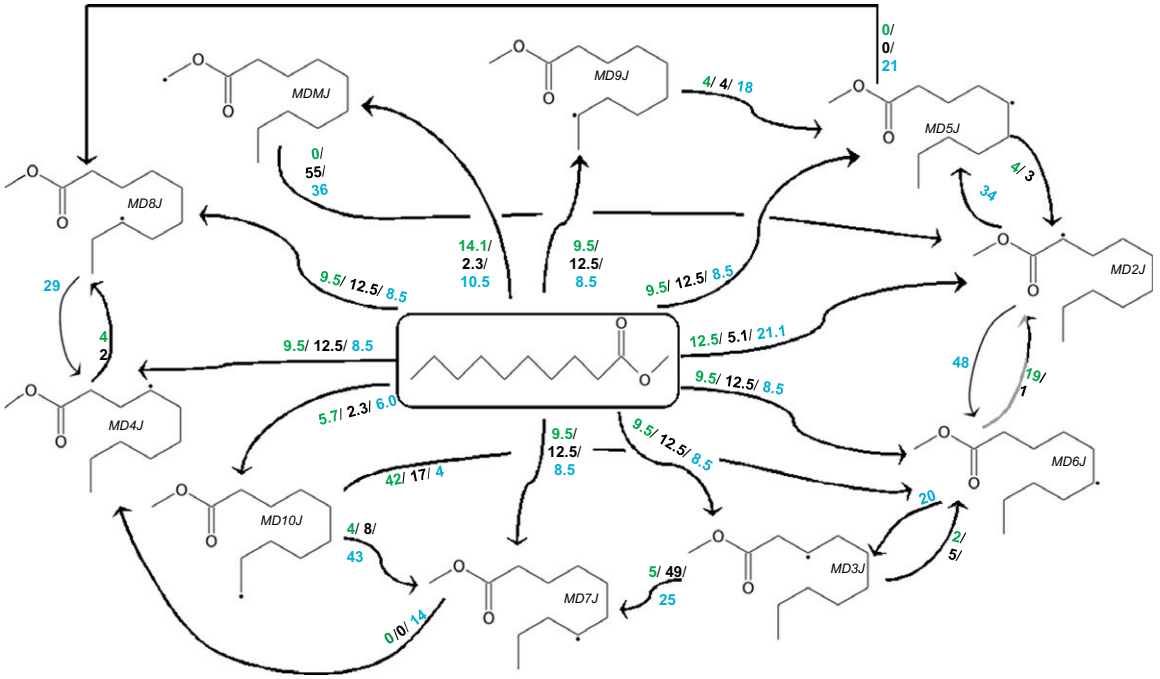

Fig. 11. Path flux analysis in a shock tube (1789/210,000/781,211 ppm MD/O_2/Ar, 7.84 atm and 1185 K [19]) at 50% MD conversion. The values in green, black and blue refer to the present detailed model, the model of Herbinet et al. [21] and the model of Glaude et al. [18] respectively. (For interpretation of the references to color in this figure legend, the reader is referred to the web version of this article.)

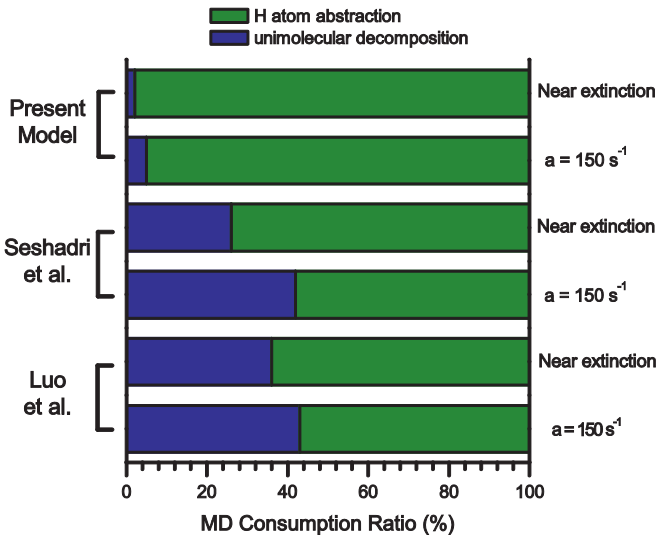

Fig. 12. Consumption pathways of methyl decanoate in a diffusion flame: differences between the present model, Seshadri et al. [16] and the Luo et al. [23].

radicals in the model of Luo et al. precludes it from a similar delineation of detailed oxidation pathways). The reduced model of Seshadri et al. does not consider the radicals MD10J ($CH_2(CH_2)_8CO_2CH_3$) and MDMJ ($C_9H_{19}CO_2CH_2$), thus assuming that a H atom abstraction from these two positions is unlikely. According to the present model nearly 13% of the fuel is converted to the MDMJ radical, and then reacts through a β-scission reaction to generate formaldehyde. However both models consider the radical MD2J ($CH_3(CH_2)_7CHCO_2CH_3$) as the main radical generated from the parent fuel. Both models agree to consider the β-scission reactions of the MD radicals as their main consumption pathways, with a minor contribution from isomerization reactions. Finally it is noteworthy that the fate of the radical ME2J (CH_3OCOCH_2) is quite different between the two models. The production rate of this radical is firstly different (directly produced from the fuel in the model of Seshadri et al.) but more interesting is its consumption paths. The present model forecast that 93% of this radical breaks apart to produce ketene and a methoxy radical, whereas in the model of Seshadri et al. 80% isomerizes to the MEMJ ($CH_3CO_2CH_2$) that further decomposes to formaldehyde and an acetyl radical.

3.3.3. Sensitivity analysis

Although not shown here, sensitivity analyses to the kinetic parameters have been performed to the computation of ignition delays, laminar flame speeds and extinction limits. The results show that all these global parameters are mainly sensitive to the chemistry of the small intermediate species (C_0 to C_3 species), and show only a weak dependence to the fuel specific chemistry. Therefore these results are not discussed in this paper as only highly detailed analyses, such as we performed previously for MB [9], may extract meaningful information with which to refine the methyl decanoate oxidation kinetics.

3.4. Conclusions on MD kinetic modeling

A model has been developed by propagating the kinetics and thermochemistry employed for MB by Dooley et al. [8] by appropriate analogy to MD. The model has then been tested against a large set of available experimental data (ignition delays, speciation profiles in JSR and counterflow diffusion flame, laminar flame speeds, extinction limits of diffusion flames) and compared to computations from previous kinetics models [16–18,21–23]. The aim in developing this model was to assess the hypothesis that propagating well performing MB kinetics to MD without modification should result in better model predictions. The presented analyses (Figs. 1, 5, 6 and 8–10) have shown that this model performs reasonably well over a large range of conditions, but shows significant differences to the performance of previous models. Significantly, the different kinetic subsets prescribed result in completely different oxidation pathways (Figs. 11–13), and therefore in the formation of a different pool of controlling intermediate species. The future experimental study of methyl ester reaction kinetics should thus focus on speciation measurements of smaller than C_6 methyl esters as model molecules with which to gain more insight on the methyl ester oxidation framework and constrain the kinetic models.

4. Similarities in the oxidation of methyl ester

As shown previously [9], and again in Fig. 9, MD exhibits a stronger resistance (on a molar basis) to extinction than the smaller ester, MB. However as discussed by Dooley et al. [9], MB and MD have different flame properties that make drawing any fair conclusions on the chemical kinetic contribution to flame reactivity very difficult. Recently Won et al. [49] studied the extinction limits of a large set of fuel components, including n-alkanes, iso-alkanes and aromatics. Motivated by this question, they suggested a new parameter, the *transport-weighted enthalpy* (TWE) as a metric in order to fairly compare the chemical kinetic, mass diffusive and potential energy contributions of different fuels to the occurrence of flame phenomena. The TWE accounts for the difference in

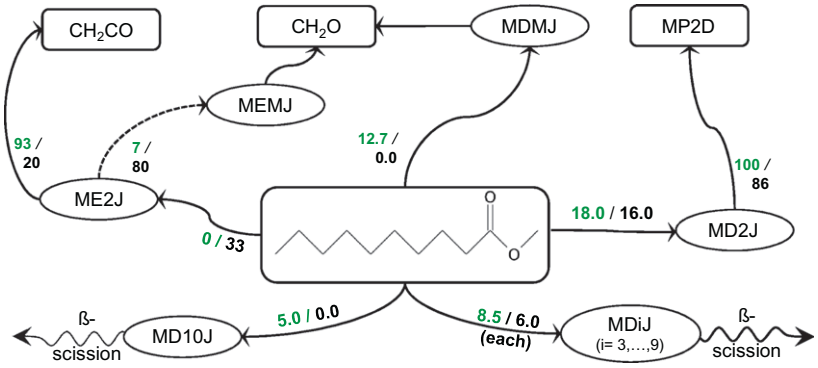

Fig. 13. Integrated path flux analysis in a MD/air counterflow diffusion flame (X_{fuel} = 0.11 and a = 150 s^{-1}). The values in green and black refer to the present reduced model and the model of Seshadri et al. [16] respectively. (Please refer to Fig. 11 for the translation of molecular formula to chemical structure.) (For interpretation of the references to color in this figure legend, the reader is referred to the web version of this article.)

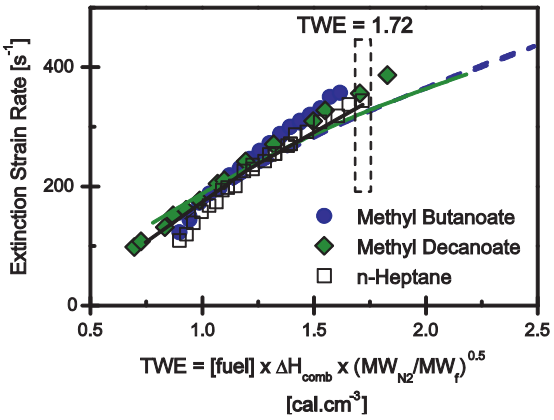

Fig. 14. Extinction strain rates of methyl butanoate (blue), methyl decanoate (green) and n-heptane (black) [9] diffusion flames versus transport-weighted enthalpy [49] (symbols are experimental data and lines model computations). (For interpretation of the references to color in this figure legend, the reader is referred to the web version of this article.)

energy content. In addition, this property cannot be separated by experiment from the rate of mass diffusion as both are inherent to molecule size. However Won et al. have shown these differences may be theoretically normalized (through the square root of the molecular weight, MW, of the fuel and by use of the enthalpies of combustion of each fuel) to decouple the kinetic contribution on diffusion flame extinction from the thermal and transport issues. MB and MD have both different molecular weight and different enthalpies of combustion. For a same fuel mole fraction, MB diffuses faster to the reaction zone due to the smaller MW (MW = 102.14 g mol^{-1} and 186.29 g mol^{-1} for MB and MD, respectively) whereas the heat of combustion of MD is higher thus resulting in a higher peak flame temperature ($\Delta H_{comb} = -704.0$ kcal mol^{-1} and -1648.6 kcal mol^{-1} for MB and MD). Transport weighted enthalpy, TWE, is defined as below [49]

$$\mathrm{TWE} = [\mathrm{fuel}] \times \Delta H_{comb} \times \sqrt{\frac{MW_{diluent}}{MW_{fuel}}} \quad (1)$$

Figure 14 shows the extinction strain rate for MB and MD as a function of TWE for both experiments and numerical computations. The extinction limits of n-heptane (nH), chosen as a representative of the n-alkanes [9], are also presented in Fig. 14. After normalization by TWE, MB and MD exhibit the same extinction behavior, as well as being very similar to that measured for nH [9]. This comparison suggests that the chemical kinetic reactivity of the three fuels at high temperatures is extremely similar. To rationalize this observation, computations were performed with the MB, MD and nH reduced models for TWE = 1.72 cal cm^{-3} (equating to mole fraction of 0.191, 0.110 and 0.115 for MB, MD and nH respectively) at the initial fuel temperature of 500 K. It is noteworthy that computations

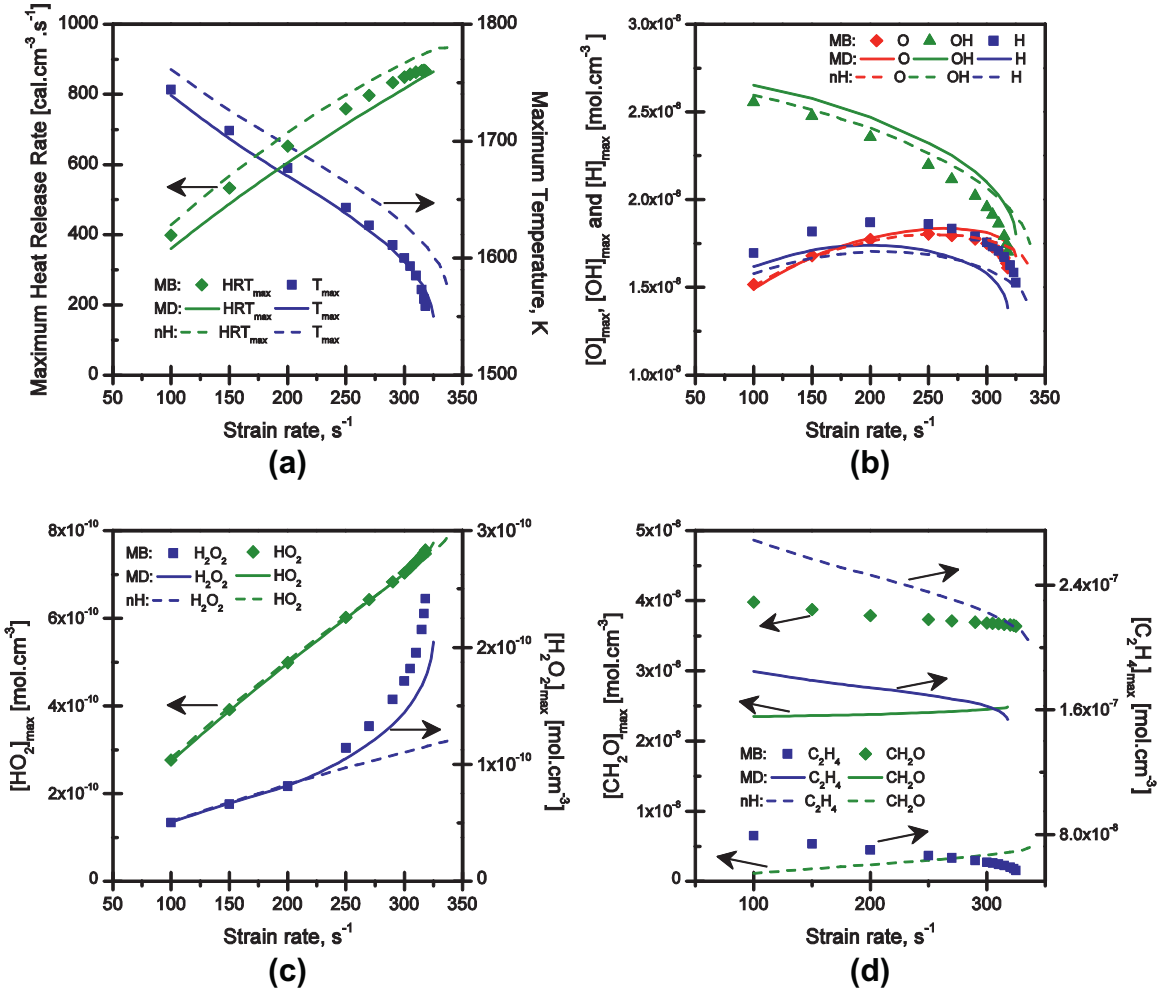

Fig. 15. Temperature and species profiles of main intermediates and radicals in an atmospheric methyl decanoate (solid line) and methyl butanoate (symbols) diffusion flame for a same *transport-weighted enthalpy*, 1.72 ($X_{MD} = 0.110$, $X_{MB} = 0.191$ and $X_{nH} = 0.115$).

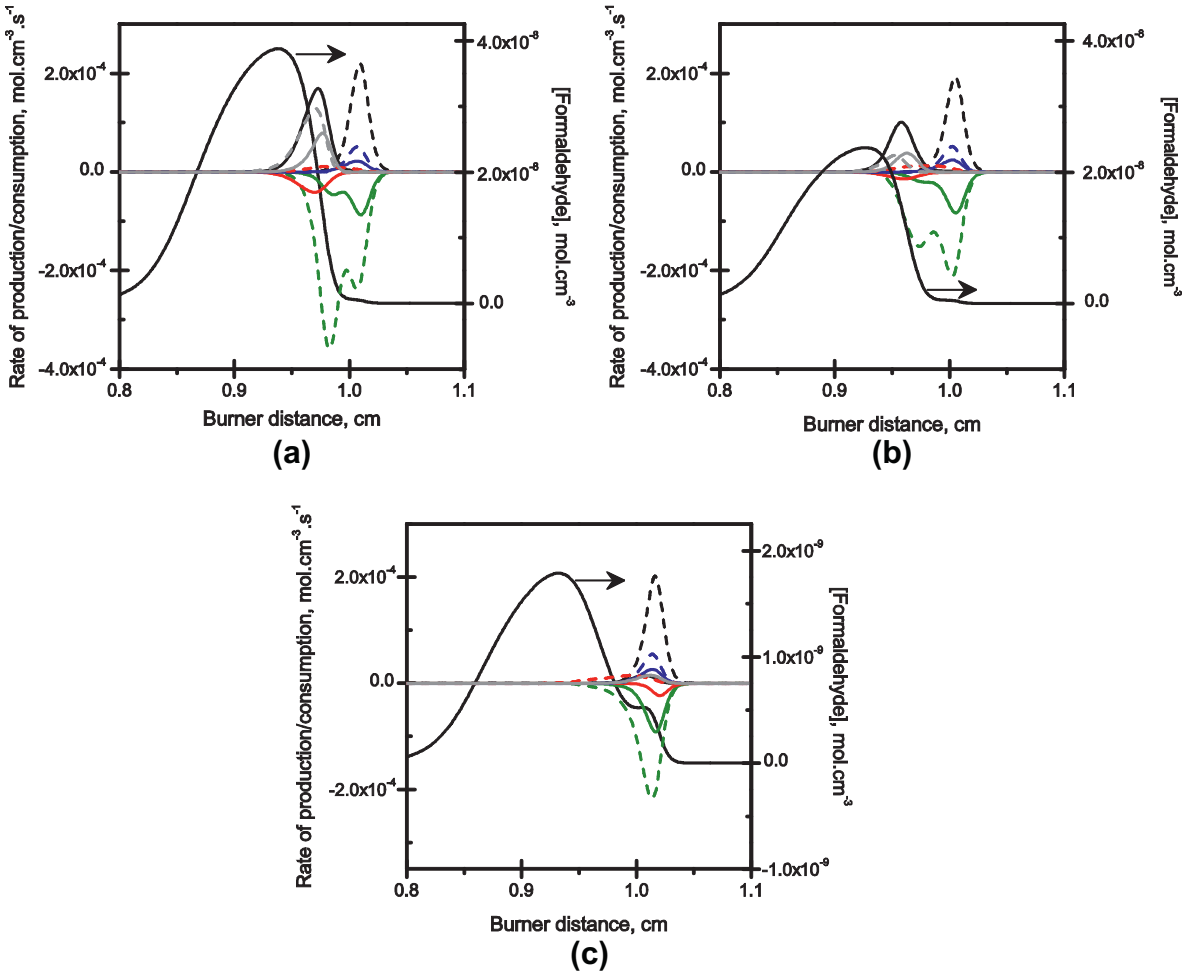

Fig. 16. Formation and consumption pathways of formaldehyde in an atmospheric counterflow fuel/air diffusion flame: TWE = 1.72, a = 150 s^{-1} and T_{fuel} = 500 K. The fuels are methyl butanoate (a) (— $CH_3O + (M) = CH_2O + H(+M)$, – – $CH_3 + O = CH_2O + H$, — $CH_2 + O_2 = CH_2O + O$, — — $CH + H_2O = CH_2O + H$, — — $C_2H_3 + O_2 = CH_2O + HCO$, — MP2DMJ = $CH_2O + C_2H_3CO$, — — MBMJ = $CH_2O + nC_3H_7CO$, — $CH_2O + OH = HCO + H_2O$, — — $CH_2O + H = HCO + H_2$, — $CH_2O + CH_3 = HCO + CH_4$), methyl decanoate (b) (— $CH_3O + (M) = CH_2O + H(+M)$, – – $CH_3 + O = CH_2O + H$, — $CH_2 + O_2 = CH_2O + O$, — — $CH + H_2O = CH_2O + H$, — — $C_2H_3 + O_2 = CH_2O + HCO$, — MP2DMJ = $CH_2O + C_2H_3CO$, — — MDMJ = $CH_2O + nC_9H_{19}CO$, — $CH_2O + OH = HCO + H_2O$, — — $CH_2O + H = HCO + H_2$, — $CH_2O + CH_3 = HCO + CH_4$) and n-heptane (c) (— $CH_2O + H(+M) = CH_2OH(+M)$, – – $CH_3 + O = CH_2O + H$, — $CH_2 + O_2 = CH_2O + O$, — — $CH + H_2O = CH_2O + H$, — — $C_2H_3 + O_2 = CH_2O + HCO$, — $CH_2OH + O_2 = CH_2O + HO_2$, — $CH_2O + OH = HCO + H_2O$, — — $CH_2O + H = HCO + H_2$, — $CH_2O + O = HCO + OH$).

with the present model also reproduce the experimental observations. Following Dooley et al. [9], Fig. 15 presents the computed concentration profiles of the main radicals (O, OH, H and HO_2), the maximum flame temperature and the heat release rate as a function of the strain rate. As expected the radical and temperature profiles are found to be nearly identical for the two biofuels and the n-alkane, whereas the profiles of the two main intermediates C_2H_4 and CH_2O (Fig. 15d) are widely different.

To understand the reasons for these differences, a flux analysis for the formation of formaldehyde in MD, MB and nH (TWE = 1.72 cal cm^{-3}, a = 150 s^{-1} and T_{fuel} = 500 K) diffusion flames is presented in Fig. 16. Similar to the analysis of methyl butanoate flames by Dooley et al. [9], the concentration of formaldehyde computed in MD fueled flames differs by almost a factor of ten from that computed in the n-alkane fuel flame. In methyl ester fueled flames, formaldehyde is produced before the core reaction zone directly from the decomposition of the methyl ester fuel fragments (from MDMJ, MP2DMJ, CH_3O and MBMJ) [9]. Then, in the core reaction zone where heat release is major, formaldehyde is produced for the three investigated fuels through reactions involving small radicals Formaldehyde reacts mainly through H abstraction reactions with H atoms and OH radicals to generate formyl radicals HCO. The formyl radical may decompose into CO and either an H atom (radical chain brancher) or a HO_2 radical (radical chain propagator), whether it reacts unimolecularly or with molecular oxygen.

The TWE analysis suggests that for a global parameter such as the diffusion extinction (and high temperature ignition delays), a methyl ester exhibits similar reactivity to that of a simple n-alkane when accounting for the necessary fuel characteristic. Actually, the extinction limits of diffusion flames are strongly dictated by the high temperature chemistry, in which the propensity to populate the radical pool is mostly governed by the kinetics of the C_0—C_2 chemistry linked to the fuel consumption pathways. Nevertheless, the similar reactivity between n-alkanes and methyl esters in the global parameters, such as diffusion flame extinction, does not necessarily imply similarities in the detailed structure of the flame, *i.e.*, the nature and concentration of the intermediate species (Figs. 15d and 16). Thus, detailed studies of methyl ester kinetic specificities need to be performed in order to improve the current kinetic model of methyl esters.

5. Concluding remarks

A detailed kinetic model for the biodiesel surrogate methyl decanoate (MD) has been developed. The model uses the chemical

reaction scheme constructed by Herbinet et al. [21] but prescribes the kinetic and thermochemical parameters developed to describe methyl butanoate (MB) oxidation. These reaction rate constants and thermochemical parameters were propagated without any modification from the MB model to all of the MD subsets. The model has been tested in an *a priori* manner and performs generally well against all experimental data (shock tubes, JSR, laminar burning velocities and diffusion flame speciation profiles and extinction limits). The overall better performance of the model demonstrates that the methodology adopted here, the similarity rule of the methyl ester moiety rather than from n-alkane kinetics, leads to improved computational predictability. However, some discrepancies of model computation to experiment are also apparent.

The computational comparison of the present model with the previous published models highlighted the influence of the input parameters, *i.e.*, thermochemical data and rate constants. Especially, the estimation of thermochemical parameters significantly affects the MD consumption pathways, and thus the model predictability. Likewise, rate constant parameters of reactions specific to the methyl ester moiety are observed to strongly impact the oxidation pathways of the parent fuel, and consequently the pool of intermediate species (CH_2O, methyl acrylate, CH_2CO) and thus also impact the model predictability. Foundational studies of thermochemical properties and kinetic parameters specific to the methyl ester moiety are presently lacking but are highlighted as a requirement for the development of reliable combustion models for methyl esters. The apparent expendability of methyl butanoate model parameters to model the oxidation of MD, places particularly emphasis on the study of smaller methyl esters as the influences specific to the methyl ester moiety ought to be more easily discernible in those systems.

Extinction limits of MB, MD and n-heptane diffusion flames were compared through a transport-weighted enthalpy [49], enabling a decoupling of kinetic effect from the issues of diffusion and enthalpy of combustion. The three fuels were observed to exhibit a similar kinetic behavior near the extinction limit when compared with this new metric. However, main intermediate concentrations (CH_2O, C_2H_4) were computed to be different for each class of fuel highlighting the methyl ester kinetics specificities. In spite of a similar kinetic potential at these high temperature conditions, n-alkanes and methyl esters exhibit unique reaction paths therefore resulting in a different population of intermediate species.

Acknowledgments

The authors acknowledge D.R. Haylett et al. of Stanford University for providing shock tube data before publication. This work is supported as part of the Combustion Energy Frontier Research Center, funded by the United States Department of Energy, office of Science, Office of Basic Energy Sciences under Award Number De-SC0001198.

Appendix A. Supplementary material

Supplementary data associated with this article can be found, in the online version, at doi:10.1016/j.combustflame.2012.01.002.

References

[1] A. Demyrbas, Prog. Energy Combust. Sci. 31 (2005) 466–487.
[2] S. Dooley, S.H. Won, M. Chaos, J. Heyne, Y. Ju, F.L. Dryer, K. Kumar, C.-J. Sung, H. Wang, M.A. Oehlschlaeger, R.J. Santoro, T.A. Litzinger, Combust. Flame 157 (2010) 2333–2339.
[3] P. Dagaut, A.E. Bakali, A. Ristori, Fuel 85 (2006) 944–956.
[4] A. Violi, S. Yan, E.G. Eddings, A.F. Sarofim, S. Granata, T. Faravelli, E. Ranzi, Combust. Sci. Technol. 174 (2002) 399–417.
[5] W.J. Pitz, N.P. Cernansky, F.L. Dryer, F.N. Egolfopoulos, J.T. Farrell, D.G. Friend, H. Pitsch, SAE Paper 2007-01-0175.
[6] E.M. Fisher, W.J. Pitz, H.J. Curran, C.K. Westbrook, Proc. Combust. Inst. 28 (2000) 1579–1586.
[7] S. Gail, M.J. Thomson, S.M. Sarathy, S.A. Syed, P. Dagaut, P. Diévart, A.J. Marchese, F.L. Dryer, Proc. Combust. Inst. 31 (2007) 305–311.
[8] S. Dooley, H.J. Curran, J.M. Simmie, Combust. Flame 153 (2008) 2–32.
[9] S. Dooley, M. Uddi, S.H. Won, F.L. Dryer, Y. Ju, Combust. Flame, in press, doi:10.1016/j.combustflame.2011.09.016.
[10] Y.L. Wang, Q. Feng, F.N. Egolfopoulos, T.T. Tsotsis, Combust. Flame 158 (2011) 1507–1519.
[11] M.H. Hakka, H. Bennadji, J. Biet, M. Yahyaoui, B. Sirjean, V. Warth, L. Coniglio, O. Herbinet, P.A. Glaude, F. Billaud, F. Battin-Leclerc, Int. J. Chem. Kinet. 43 (2011) 204–218.
[12] K. HadjAli, M. Crochet, G. Vanhove, M. Ribaucour, R. Minetti, Proc. Combust. Inst. 32 (2009) 239–246.
[13] G. Dayma, S. Gail, P. Dagaut, Energy Fuel 22 (2008) 1469–1479.
[14] G. Dayma, C. Togbé, P. Dagaut, Energy Fuel 23 (2009) 4254–4268.
[15] C. Togbé, J.-B. May-Carle, G. Dayma, P. Dagaut, J. Phys. Chem. A 114 (2010) 3896–3908.
[16] K. Seshadri, T. Lu, O. Herbinet, S. Humer, U. Niemann, W.J. Pitz, R. Seiser, C.K. Law, Proc. Combust. Inst. 32 (2009) 1067–1074.
[17] S.M. Sarathy, M.J. Thomson, W.J. Pitz, T. Lu, Proc. Combust. Inst. 33 (2010) 399–405.
[18] P.A. Glaude, O. Herbinet, S. Bax, J. Biet, V. Warth, F. Battin-Leclerc, Combust. Flame 157 (2010) 2035–2050.
[19] D.R. Haylett, D.F. Davidson, R.K. Hanson, Combust. Flame 159 (2012) 552–561.
[20] W. Wang, M.A. Oehlschlaeger, Combust. Flame 159 (2012) 476–481.
[21] O. Herbinet, W.J. Pitz, C.K. Westbrook, Combust. Flame 154 (2008) 507–528.
[22] O. Herbinet, W.J. Pitz, C.K. Westbrook, Combust. Flame 157 (2010) 893–908.
[23] Z. Luo, T. Lu, M.J. Maciaszek, S. Som, D.E. Longman, Energy Fuel. 24 (2010) 6283–6293.
[24] A. Farooq, D.F. Davidson, R.K. Hanson, L.K. Huynh, A. Violi, Proc. Combust. Inst. 32 (2009) 247–253.
[25] D. Healy, D.M. Kalitan, C.J. Aul, E.L. Petersen, G. Bourque, H.J. Curran, Energy Fuel 24 (2010) 1521–1528.
[26] A.M. El-Nahas, M.V. Navarro, J.M. Simmie, J.W. Bozzelli, H.J. Curran, S. Dooley, W. Metcalfe, J. Phys. Chem. A 111 (2007) 3727–3739.
[27] A. Osmont, L. Catoire, I. Gökalp, M.T. Swihart, Energy Fuel 21 (2007) 2027–2032.
[28] A. Osmont, L. Catoire, P. Dagaut, J. Phys. Chem. A 114 (2010) 3788–3795.
[29] R. Sumathi, W.H. Green, Phys. Chem. Chem. Phys. 5 (2003) 3402–3417.
[30] S.W. Benson, in: Thermochemical Kinetics, Wiley, New York, 1976.
[31] E.R. Ritter, J.W. Bozzelli, Int. J. Chem. Kinet. 23 (1991) 767–778.
[32] A.Y. Chang, J.W. Bozzelli, A.M. Dean, Z. Phys. Chem. 214 (2000) 1533–1568.
[33] C. Sheng, J.W. Bozzelli, A.M. Dean, A.Y. Chang, J. Phys. Chem. A 106 (2002) 7276–7293.
[34] S.M. Villano, L.K. Huynh, H.-H. Carstensen, A.M. Dean, in: Proc. 7th US National Meeting, 2011, Paper 1A05.
[35] J.D. De Sain, S.J. Klippenstein, J.A. Miller, C.A. Taatjes, J. Phys. Chem. A 107 (2003) 4415–4427.
[36] C.J. Hayes, D.R. Burgess Jr., Proc. Combust. Inst. 32 (2009) 263–270.
[37] R. Asatryan, J.W. Bozzelli, J. Phys. Chem. A 114 (2010) 7693–7708.
[38] A. McClellan, Tables of Experimental Dipole Moments, Freeman, San Francisco, 1963.
[39] R. Bosque, J. Sales, J. Chem. Inform. Comput. Sci. 42 (2002) 1154–1163.
[40] W. Sun, Z. Chen, X. Gou, Y. Ju, Combust. Flame 157 (2010) 1298–1307. http://engine.princeton.edu/.
[41] P. Glarborg, R.J. Kee, J. Grcar, J.A. Miller, PSR: A FORTRAN Program for Modeling Well-Stirred Reactors, Sandia National Laboratories, SAND86-8209, 1986.
[42] R.J. Kee, G. Dixon-Lewis, J. Warnatz, M.E. Coltrin, J.A. Miller, Technical Report SAND86-8246, Sandia National Laboratories, Albuquerque, NM, 1986.
[43] R.J. Kee, F.M. Rupley, J.A. Miller, Chemkin II: A FORTRAN Chemical Kinetics Package for the Analysis of a Gas-phase Chemical Kinetics, SAND89-8009B, Sandia Laboratories, 1993.
[44] A.E. Lutz, R.J. Kee, J.F.Grcar, F.M. Rupley, OPPDIF: A FORTRAN Program for Computing Opposed-Flow Diffusion Flames, SAND96-8243, Sandia Laboratories, 1997.
[45] R.J. Kee, A.E. Lutz, F.M. Rupley, et al., Premix: A Program for Modeling Steady, Laminar, One-dimensional Premixed Flames, Reaction Design Inc., 2000.
[46] D. Goodwin, Cantera: Object-Oriented Software for Reacting Flows, California Institute of Technology, 2005. <http://sourceforge.net/projects/cantera>.
[47] S. Jahangirian, S. Dooley, F.M. Haas, F.L. Dryer, Combust. Flame 159 (2012) 30–43.
[48] B.G. Sarnacki, G. Esposito, R.H. Krauss, H.K. Chelliah, Combust. Flame, in press. doi:10.1016/j.combustflame.2011.09.007.
[49] S.H. Won, S. Dooley, F.L. Dryer, Y. Ju, Combust. Flame 159 (2012) 541–551.